Beyond Cargo Hitching

Combined People and Freight Transport Using Dynamically Configurable Autonomous Vehicles

Kortekaas, Joris J.A.; Beirigo, Breno A.; Schulte, Frederik

DOI
10.1007/978-3-031-43612-3_24

Publication date
2023

Document Version
Final published version

Published in
Computational Logistics

Beyond Cargo Hitching: Combined People and Freight Transport Using Dynamically Configurable Autonomous Vehicles

Joris J. A. Kortekaas[2], Breno A. Beirigo[1], and Frederik Schulte[2(✉)]

[1] Department of High-tech Business and Entrepreneurship, University of Twente, Hallenweg 17, 7522 NH Enschede, The Netherlands
b.alvesbeirigo@utwente.nl

[2] Department of Maritime and Transport Technology, Delft University of Technology, Mekelweg 2, 2628 CD Delft, The Netherlands
j.j.a.kortekaas@student.tudelft.nl, f.schulte@tudelft.nl

Abstract. A *Dynamically Configurable Autonomous Vehicle* (DCAV) is a new class of autonomous vehicle concept using a separable design of lower and upper parts—carriers and modules—to allow more flexible operation. A fleet of DCAVs consists of a set of carriers and a set of compatible modules. Different, possibly crowd-sourced, modules can increase the number of use-cases for DCAVs, possibly leading to disruptive changes in the transport sector. This study investigates the use of DCAV system operating on an *Autonomous Mobility-on-Demand* (AMoD) scenario, combining passenger and freight transport flows. The novel problem is denoted as the *Dynamically Configurable Autonomous Vehicle Pickup and Delivery Problem* (DCAVPDP). We propose a *mixed-integer linear programming* (MILP) model aiming to minimize DCAV-fleet size and distance traveled. We compare the performance of a DCAV fleet to the performance of a typical single-purpose fleet (consisting of dedicated passenger and freight vehicles). The numerical study, with 360 instances for each fleet type, considering four people-and-freight demand distribution scenarios, the inclusion of ridesharing, module-and-carrier (de)coupling locations, and different simulation horizon lengths, shows that the proposed modular DCAV system can fulfill a mixed people-and-freight demand using, on average, 18.77% fewer carriers than a regular AMoD system comprised of single-purpose vehicles while increasing on-duty fleet utilization by 4.82%.

Keywords: Dynamically Configurable Autonomous Vehicles · Shared Autonomous Vehicles · Cargo Hitching · Combined Passenger and Freight Transport · Ridesharing

1 Introduction

Dynamically Configurable Autonomous Vehicles (DCAVs) are a new class of autonomous vehicles using a separable design concept consisting of drive and transport units. The drive unit (also called the carrier, driveboard, or chassis)

J. R. Daduna et al. (Eds.): ICCL 2023, LNCS 14239, pp. 381–395, 2023.
https://doi.org/10.1007/978-3-031-43612-3_24

is a standardized platform housing self-driving equipment (e.g., sensors, motors, battery). The transport unit (also referred to as module, capsule, pod, or body) is a switchable add-on part that can be dynamically and autonomously outfitted onto drive units to accommodate any commodity type (see Fig. 1). Such a modular nature of DCAVs increases operational flexibility, enabling various use-cases: transport providers can assign diverse modules to carriers to fulfill different demands.

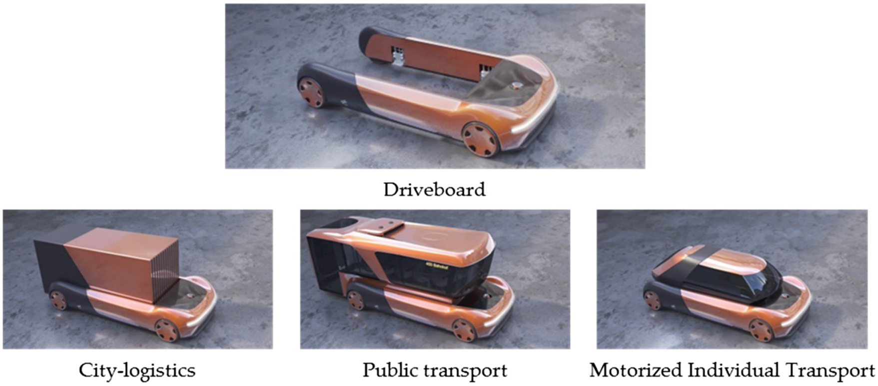

Fig. 1. Example of a Dynamically Configurable Autonomous Vehicle (DCAV) system [15]. The drive unit (carrier) can autonomously outfit diverse transport units (modules) on the fly to service heterogeneous demands such as freight and mobility.

By separating drive and transport units, providers can increase the utilization of self-driving carriers (presumably, the most expensive assets) while increasing profits, adapting to changing demand profiles such as people and freight on the operational level. Typically, vehicle acquisition is a long-term investment, which makes deciding on adequate fleet size and mix a complex strategical decision [2,7]. Therefore, relying on a DCAV fleet may also mitigate losses due to drastic demand shifts. For example, the COVID outbreak led to a surge in delivery services while social distancing decreased mobility, exposing the fragility of transportation systems based on single-purpose vehicles [12]. Ultimately, investing in additional freight modules to accommodate a higher freight demand is expected to be considerably cheaper than investing in entirely new freight vehicles.

Combined people and freight transportation systems have been gaining attention in the literature [3,9]. For example, solution approaches have been designed for settings where people and parcel share rides on taxis (see, e.g., [8]) and compartmentalized autonomous vehicles (see e.g., [1,13]). However, there is no study on optimizing the operations of a DCAV-based transportation system that dynamically switches transport units to fulfill heterogeneous demand. Only concept designs have been evaluated (see, e.g., [10,11,15]) and presented by companies such as the Continental BEE [4], the Mercedes Benz Vision Urbanetic [5] and the Toyota e-palette [14].

This study presents a *mixed-integer linear programming* (MILP) formulation for the *Dynamically Configurable Autonomous Vehicle Pickup and Delivery Problem* (DCAVPDP) arising on a transport system that services both passenger and freight demands. Our formulation extends the formulation by [6] for the *vehicle routing problem with trailers and transshipments* (VRPTT) by adding service level constraints as formulated in *dial-a-ride problems* (DARPs). Additionally, we consider the integration of passenger and freight transport, the use of parking locations, and allowing multiple trips and ridesharing. The model seeks to find an optimal routing solution that minimizes vehicle utilization in terms of linear combination of the distance traveled by carriers and modules.

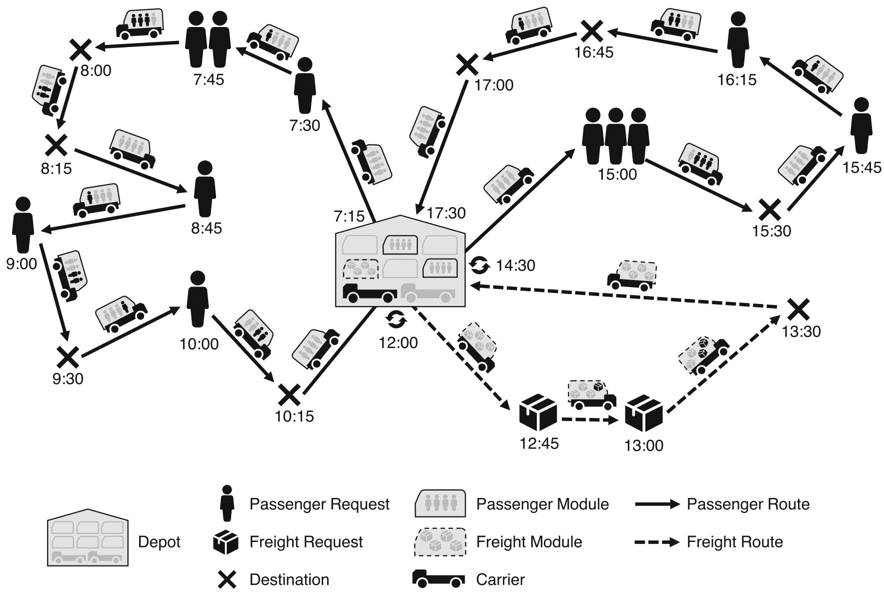

Fig. 2. Example of a DCAV fleet operation throughout a typical day.

Figure 2 shows an operational example of a DCAV fleet using different modules throughout the day to fulfill passenger and freight requests. The carrier starts at 7:15 at the depot and couples a passenger module to transport passengers during the morning rush hour. As long as the vehicle capacity is not exceeded, the vehicle is allowed to make multiple pickups and have passengers share the ride. When the latest passenger of the first trip is dropped off at 10:15 the vehicle gets called back to the depot. Next, the carrier switches its passenger module for a freight module and starts servicing freight requests as demand for passenger transport is low at the time. After picking up several packages the vehicle returns to the depot once more at 14:30 to switch over to a passenger module to transport passengers for the remainder of the afternoon. To meet demand the carrier has made three separate trips to and from the depot, changing modules for each trip. Even though demand fluctuates throughout the day, the carrier is being used to serve requests for either passengers or parcels, resulting in high carrier utilization.

We benchmark the performance of the DCAV fleet (consisting of carriers and passenger and freight modules) with a typical single-purpose fleet (consisting of dedicated passenger and freight vehicles). We consider carriers and dedicated vehicles of modular and single-purpose fleets have to start and end their route at a central depot. Vehicles are not allowed to arrive early and wait at a pickup location since requests are made on-demand, and there is little room for parking in city centers. However, parking locations are available for vehicles to wait until a pickup is requested; these locations can also be used for modular vehicles to switch modules. In contrast, modules do not have to start or end their route at the depot. They can also start and end their route from a parking location and do not have to return to the same location as where they originated from. We assume there is no limit to the number of times a module can be switched, except occupied modules, which are not allowed to be switched.

2 Problem Description

This study considers a *Dynamically Configurable Autonomous Vehicle Pickup and Delivery Problem* (DCAVPDP), which focuses on the daily operations of an on-demand transportation provider that uses a DCAV fleet to pick up and deliver requests of both passengers and parcels. We assume carriers are required to start and end their route at a central depot and are not allowed to arrive early and wait at a request location—there is little room for parking in an urban city environment. However, parking locations are available for vehicles to wait until a pickup is requested. These locations can also be used for modular vehicles to switch modules. Modules do not have to start or end their route at the depot and can be repeatedly switched when empty. Ridesharing is allowed between requests of the same commodity, with detours limited by maximum extra ride times.

Figure 3 highlights the difference between a modular and a single-purpose fleet when servicing one passenger and one freight request. The single-purpose fleet uses two dedicated vehicles traveling direct routes from the depot to the pickup and delivery. In contrast, the DCAV fleet uses available parking locations to gather modules closer to request locations and uses a single carrier to service both requests. The carrier leaves the depot and travels to a parking location where it couples a freight module to service the freight request. After reaching the destination of the freight request, it drives to another parking location to decouple the freight module and travel to the final available parking location to couple a passenger module. The passenger module is used to service the passenger request and returns together with the carrier to the depot.

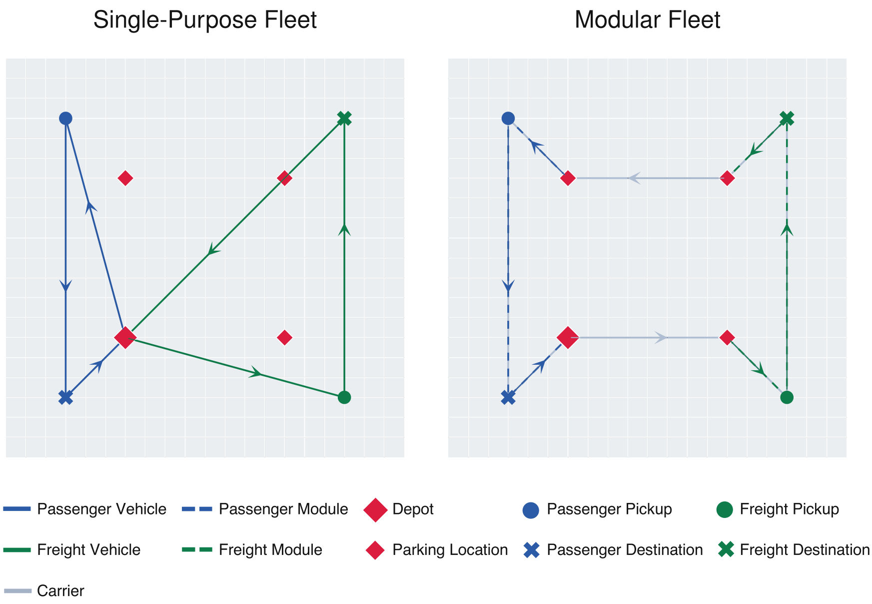

Fig. 3. Difference between single-purpose and modular DCAV fleets when servicing the same passenger and freight request set.

3 Problem Formulation

The DCAVPDP is defined on a directed graph $G = (V, A)$, consisting of vertices V and arcs A, and requires synchronisation in time and space of the movement of carriers and modules. We consider a grid service area where a total number of n_r requests is generated. The set of all vehicles is indicated by F, which is a collection of all vehicles that are available to the model. The set of all vehicles is further separated in the sets F_{a}, F_{q}, and F_{m}. All motorized vehicles in the model are indicated by F_{a}, which is a combination of all passenger and freight vehicles and the carriers. F_{q} is the set of all vehicles that have load-carrying capability, which consists of the passenger and freight vehicles and the passenger and freight modules. The final set regarding vehicles is F_{m}, which is a set of all modules in the model. Where V^k are all reachable vertices for vehicle k, V_{P}^k is a set of all reachable pickup vertices for vehicle $k \in F$.

The set of traversable arcs A^k is further specified in the following sets: A_{C}^m, A_{PD}^k, and A_{W}^k. The set A_{C}^m describes all traversable arcs module $m \in F_{\mathrm{m}}$ can travel along when being coupled to carrier $c \in C$, since modules are not capable of traveling between real-world locations without the assistance of a carrier. However, modules are allowed to travel to couple vertices on their own to allow for the distribution of modules across all parking locations. The number of parking locations in the model is specified by n_{p} and f and 0 correspond to the start and final vertex respectively. This ensures a module can be coupled at all available parking locations on the grid after being decoupled from a carrier. A_{PD}^k

Table 1. Sets, parameters, and variables of the DCAVPDP and dedicated people and freight integrated problem.

Sets	
$C, M_\mathrm{p}, M_\mathrm{f}$	Carriers and passenger and freight modules (modular fleet)
$K_\mathrm{p}, K_\mathrm{f}$	Passenger and freight vehicles (dedicated fleet)
F	$= K_\mathrm{p} \cup K_\mathrm{f} \cup C \cup M_\mathrm{p} \cup M_\mathrm{f}$. Set of all vehicles (fleet)
F_a	$= K_\mathrm{p} \cup K_\mathrm{f} \cup C$. Set of powered vehicles (autonomous)
F_q	$= K_\mathrm{p} \cup K_\mathrm{f} \cup M_\mathrm{p} \cup M_\mathrm{f}$. Set of vehicles with load carrying capability
F_m	$= M_\mathrm{p} \cup M_\mathrm{f}$. Set of all modules
V^k	Set of all reachable vertices for vehicle $k \in F$
V_P^k	Set of all reachable pickup vertices for vehicle $k \in F$
V_P	$= \bigcup_{k \in F} V_p^k$
V_park^k	Set of all vertices where vehicle k is allowed to wait
A^k	Set of all traversable arcs for vehicle $k \in F$
A_C^m	Set of arcs module $m \in F_\mathrm{m}$ can only traverse while spatially synchronised with a compatible carrier $c \in C$
A_PD^k	Set of traversable arcs between request pairs for vehicle $k \in F$
A_W^k	Set of arcs for vehicle $k \in F$ where waiting is not allowed at the arrival vertex
Parameters	
Vehicles	
n_k	Number of available vehicles with load carrying capability
n_c	Number of available carriers
Q^k	Capacity of vehicle $k \in F$
v^k	Speed of vehicle $k \in F$
Requests	
n_r	Number of requests
q_i	Demand of request at vertex $i \in V_\mathrm{P}$
e_i	Earliest pick up time of request at vertex $i \in V_\mathrm{P}$
δ_i	Maximum waiting time of request at vertex $i \in V_\mathrm{P}$
Δ_i	Maximum extra ride time of request at vertex $i \in V_\mathrm{P}$
Model	
0	Start vertex for all vehicles
f	Final vertex for all vehicles
n_p	Number of parking locations
s_i	Service time at vertex $i \in V$
$d_{i,j}$	Travel distance from vertex i to vertex j
$t_{i,j}$	Travel time from vertex i to vertex j
w_m	Weight of module travel distances
$w_{rejection}$	Requests rejection penalty
S	Simulation start time
H	Simulation horizon
Variables	
$x_{i,j}^k$	(Binary) 1 if vehicle k traverses arc (i, j), 0 otherwise
τ_i^k	Arrival time of vehicle k at vertex i
ω_i^k	Load of vehicle k after vertex i
r_i^k	Ride time of request i on vehicle k

is a set of traversable arcs for vehicle $k \in F$ that are composed of a pickup and delivery pair. Finally, A^k_{W} is a set of traversable arcs for vehicle $k \in F$ on which arriving early is not allowed since vehicles are not allowed to wait at request locations.

The total number of requests in the model is specified by n_{r}. Each request has a pickup vertex $i \in V_{\mathrm{P}}$, which has a demand size of q_i. The corresponding delivery vertex has a demand size of $-q_i$, effectively emptying the vehicle again. The pickup time window of request i is determined by the earliest pickup time e_i of the request and its maximum waiting time δ_i. The earliest pickup times of requests are being generated during simulation horizon H, starting from simulation start time S. Requests do not have a set delivery time window, instead, each request has a maximum extra ride time Δ_i. The destination of a request has to be reached within the sum of the travel time and the maximum extra ride time. Additionally each vertex $i \in V$ has a service duration of s_i seconds. n_{k} specifies the number of available vehicles in the model that have a load-carrying capability (passenger and freight vehicles as well as passenger and freight modules), while n_{c} specifies the number of carriers available to the model. All vehicles have a set capacity of Q^k and an average speed of v^k. Table 1 shows an overview of all sets and parameters used in the mixed-integer linear programming model.

The formulation of the MILP is as follows:

Minimize:

$$\sum_{k \in F_{\mathrm{a}}} \sum_{(i,j) \in A^k} x^k_{i,j} d_{i,j} + w_m \sum_{k \in F_{\mathrm{m}}} \sum_{(i,j) \in A^k} x^k_{i,j} d_{i,j}$$
$$- \sum_{k \in F_{\mathrm{a}}} x^k_{0,f} + \sum_{i \in V_{\mathrm{P}}} (1 - \sum_{k \in F_{\mathrm{q}}} \sum_{(i,j) \in A^k} x^k_{i,j}) * w_{rejection} \tag{1}$$

Subject to:

$$\sum_{k \in F_{\mathrm{q}}} \sum_{(i,j) \in A^k} x^k_{i,j} \leq 1 \qquad \forall i \in V_{\mathrm{P}} \tag{2}$$

$$\sum_{(i,h) \in A^k} x^k_{i,h} - \sum_{(h,j) \in A^k} x^k_{h,j} = 0 \qquad \forall (i,j) \in A^k_{\mathrm{PD}},\ \forall k \in F_{\mathrm{q}} \tag{3}$$

$$\sum_{0,j \in A^k} x^k_{0,j} = 1 \qquad \forall k \in F \tag{4}$$

$$\sum_{i,\mathrm{f} \in A^k} x^k_{i,\mathrm{f}} = 1 \qquad \forall k \in F \tag{5}$$

$$\sum_{(h,i) \in A^k} x^k_{h,i} - \sum_{(i,j) \in A^k} x^k_{i,j} = 0 \qquad \forall i \in V^k \backslash \{0, \mathrm{f}\},\ \forall k \in F \tag{6}$$

$$x^m_{i,j} - \sum_{k \in C} x^k_{i,j} = 0 \qquad \forall (i,j) \in A^m_{\mathrm{C}},\ \forall m \in F_{\mathrm{m}} \tag{7}$$

$$x^k_{i,j} = 1 \Rightarrow \tau^m_j \leq \tau^k_j \qquad \forall (i,j) \in A^m_{\mathrm{C}},\ \forall k \in C,\ \forall m \in F_{\mathrm{m}} \tag{8}$$

$$x^m_{i,j} = 1 \Rightarrow \tau^k_j \leq \tau^m_j \qquad \forall (i,j) \in A^m_{\mathrm{C}},\ \forall k \in C,\ \forall m \in F_{\mathrm{m}} \tag{9}$$

$$\tau^k_j \geq (\tau^k_i + s_i + t_{i,j}) x^k_{i,j} \qquad \forall (i,j) \in A^k,\ \forall k \in F \tag{10}$$

$$e_i \leq \tau^k_i \leq e_i + \delta_i \qquad \forall i \in V^k_{\mathrm{P}},\ \forall k \in F \tag{11}$$

$$\tau^k_j \geq \tau^k_i \qquad \forall (i,j) \in A^k_{\mathrm{PD}},\ \forall k \in F_{\mathrm{q}} \tag{12}$$

$$x^k_{i,j} = 1 \Rightarrow \tau^k_j - \tau^k_i \leq t_{i,j} + s_i \qquad \forall (i,j) \in A^k_{\mathrm{W}},\ \forall k \in F \tag{13}$$

$$r^k_i \geq \tau^k_j - \tau^k_i \qquad \forall (i,j) \in A^k_{\mathrm{PD}},\ \forall k \in F_{\mathrm{q}} \tag{14}$$

$$t_{i,j} \leq r^k_i \leq t_{i,j} + \mathit{\Delta}_i \qquad \forall (i,j) \in A^k_{\mathrm{PD}},\ \forall k \in F_{\mathrm{q}} \tag{15}$$

$$\omega^k_j \geq \omega^k_i + q_i x^k_{i,j} \qquad \forall (i,j) \in A^k,\ \forall k \in F_{\mathrm{q}} \tag{16}$$

$$max(0, q_i) \leq \omega^k_i \leq Q_k \qquad \forall i \in V^k,\ \forall k \in F_{\mathrm{q}} \tag{17}$$

$$\omega^k_i \leq 0 \qquad \forall i \in V^k_{\mathrm{park}},\ k \in F \tag{18}$$

$$x^k_{i,j} \in \{0,1\} \qquad \forall i,j \in A^k,\ \forall k \in F \tag{19}$$

$$\tau^k_i \in \mathbb{N} \qquad \forall i \in V^k \tag{20}$$

$$\omega^k_i \in \mathbb{N} \qquad \forall i \in V^k \tag{21}$$

$$r^k_i \in \mathbb{N} \qquad \forall i \in V_{\mathrm{P}} \tag{22}$$

The objective function (1) aims to minimize the travel distance of all motorized vehicles, as well as the total number of motorized vehicles used to find an optimal solution. Secondly, the travel distance of modules is also minimized, however, it is deemed less important and is offset by a factor of w_m. To allow the model to reject requests a penalty of $w_{rejection}$ is added if a pickup vertex is not visited. Constraints (2) to (6) are the general routing constraints, and (7) to (9) are spatial and temporal synchronisation constraints to couple the movement of carriers and modules. The time window constraints are described by constraints (10) to (13) and subsequently constraints (14) and (15) are the ride time constraints. Finally, constraints (16) to (18) are the vehicle load constraints. Equations (19) to (22) describe the decision variables in the model. Constraint (2) ensures that every request's pickup vertex is visited by at most one vehicle, however, every vertex does not need to be visited. A vehicle that has visited the pickup vertex of a request must also travel to the request's destination vertex, which is ensured by (3). Constraints (4) and (5) guarantee that every vehicle starts it's route at the start vertex and ends at the final vertex respectively. To preserve flow conservation, constraint (6) enforces every vehicle to leave the same vertex it has entered. Constraint (7) is a spatial synchronisation constraint to ensure modules are only able to traverse arcs between two different real-world locations (A^m_{C}) while being coupled with a carrier. Constraints (8) and (9) are temporal synchronisation constraints that impose identical arrival times of coupled carriers and modules. The arrival time of vehicles is defined by constraint (10). Constraint (11) ensures that a request is picked up after their earliest pick-up time and within their maximum waiting time. A vehicle should arrive at the destination vertex of a request pair after the pickup vertex has been visited, which is guaranteed by (12). Vehicles are not allowed to arrive early and wait at request pickup locations, constraint (13) ensures that for the set of arcs on which waiting is not allowed (A^k_{W}) vehicles won't arrive before the earliest pickup time. Constraint (14) defines the ride time of a request, and (15) makes sure the maximum extra ride time of a request is not exceeded. Constraint (16) defines the vehicle load and (17) enforces the load of a vehicle not to exceed the maximum capacity of the vehicle. Constraint (18) guarantees that vehicles are empty when arriving at parking or decoupling vertices, to ensure no occupied vehicles or modules are parked or decoupled. Finally, constraints (19) to (22) define the model's decision variables, which are the traversed arcs, arrival time, vehicle load and ride time variables respectively.

4 Numerical Study

In this section, the configuration of the MILP for the different instances will be discussed, as well as the generation of the passenger and freight request data. Next, the general parameters of the model will be given, followed by a discussion of key performance indicators of the transport systems.

4.1 Instance Design

We test the model on two fleet configurations (viz., single-purpose and DCAV fleets) using the same request data. We consider four different demand scenarios throughout the simulation horizon H:

- **Balanced scenario (BLS)**: Both request types are uniformly distributed over the horizon.
- **Passenger peak scenario (PPS)**: Passenger requests are generated during the first half of the horizon, while freight requests are uniformly distributed throughout the whole horizon.
- **Freight peak scenario (FPS)**: Freight requests appear only during the second half of the simulation horizon, while passenger requests are uniformly distributed.
- **Complementary scenario (COS)**: Passenger requests appear during the first half of the horizon and freight requests during the second half.

Besides, we test the effect of allowing **ridesharing** (same commodity requests can share a ride) and vary the **number of parking locations** n_{p} (0, 1, or 3), where carriers can park and switch modules during their route. We also determine 15 value combinations for **simulation horizon** $H \in \{1, 8\}$, the **total fleet size** $n_{\mathrm{k}} \in \{2, 4, 6\}$, and the **number of requests** $n_{\mathrm{r}} \in \{4, 8, 12, 16, 24\}$.

Values n_{k} and n_{r} are divided equally between passenger and freight vehicles and requests, respectively. Additionally, for each module in the model, there is a carrier available to be used, thus, the number of carriers n_{c} is equal to the number of vehicles n_{k}. In the worst-case scenario, the DCAV fleet could behave similarly to the single-purpose fleet by assigning a module to each carrier and having the same routes as the single-purpose vehicles. The parameter groups $(H, n_{\mathrm{k}}, n_{\mathrm{n}})$ are as follows: $(1,2,4)$, $(1,2,8)$, $(1,2,12)$, $(1,4,4)$, $(1,4,8)$, $(1,4,12)$, $(1,6,4)$, $(1,6,8)$, $(1,6,12)$, $(8,2,12)$, $(8,2,16)$, $(8,2,24)$, $(8,4,12)$, $(8,4,16)$, $(8,4,24)$.

An overview of the 720 instances generated can be found in Fig. 4.

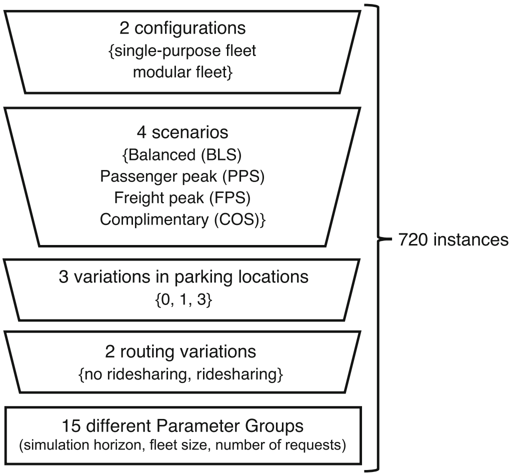

Fig. 4. Instances for the DCAVPDP and the benchmark single-purpose problem (dedicated vehicles for each commodity).

4.2 Model Parameters

The values of general parameters are shared by all instances. The grid on which the requests are being generated is $2,000$ by $2,000$ meters, with a distance between nodes of 100 m. The depot is located at (600 m, 600 m), and the three available parking locations are located at (600 m, 1400 m), (1400 m, 600 m), and (1400 m, 1400 m). When only one parking location is accessible for the fleet, it is located at (1400 m, 1400 m).

The locations of all request pickup and delivery locations are uniformly distributed over the rest of the nodes of the grid. Each request demands the transportation of one passenger or parcel (i.e., request size $q_i = 1$). Passenger and freight requests have different values for maximum waiting time δ_i, extra ride time Δ_i, and service duration s_i. All distances are calculated using the Manhattan distance formula and travel times are calculated using an average vehicle speed $v^k = 5$ m/s. To ensure vehicles will be able to reach the first request on time, we set the simulation start time $S = 900$ s since the longest possible travel time between opposing corners of the grid is 800 s. Passenger and freight vehicles and modules have a capacity $Q^k = 2$ for both the single-purpose and the DCAV fleet, respectively. Typically, passengers are more sensitive to waiting times and extra ride times, this is reflected in the model by giving more strict values to passenger requests. The maximum waiting time δ_i for passenger requests is 300 s and the maximum extra ride time Δ_i is 900 s. For freight requests, $\delta_i = 900$ s and $\Delta_i = 1800$ s. Regarding the service duration s_i, we assume a vehicle has to wait 120 s when servicing passengers and 300 s when picking up a parcel. Besides, we consider the modular DCAV fleet has an additional service duration $s_i = 120$ s to switch (i.e., couple or decouple) modules. Finally, rejecting requests incurs a penalty $w_{penalty} = 10^5$ and the traveling of modules is weighted down using $w_m = 10^{-3}$.

4.3 Performance Metrics

Our numerical study aims to assess whether a fleet of DCAVs improves vehicle utilization and occupancy while maintaining an equivalent service quality compared to a traditional single-purpose fleet. In order to highlight the differences between these two fleets, we consider the following fleet management performance metrics:

- **Utilization rate (on-duty)**: The time a vehicle is being actively used to service requests (i.e., traveling to pick up and deliver, service times at request locations), divided by the total simulation run time.
- **Utilization rate (total)**: Total time vehicles spent traveling divided by the total simulation run time. For the DCAV fleet, this time includes trips to parking locations to (de)couple modules and module replacement times.
- **Occupancy rate**: The fraction of the utilization time that vehicles are traveling loaded, taking into account their occupation ratio.
- **Service quality**: The service rate, the average pickup time of requests, and the average ride time of requests.
- **Fleet size**: Total number of autonomous vehicles (dedicated AVs or carriers).
- **Fleet capacity**: Total number of people-and-freight transportation upper parts. In the dedicated fleet, fleet capacity equals fleet size.
- **Distance traveled**: Total distance traveled by the whole fleet.

4.4 Computational Settings

The numerical study has been performed on an AMD Ryzen 5 3600 4Ghz CPU with access to 32GB of RAM. Python version 3.8.8 and commercial solver Gurobi Optimizer 9.1.2 were used to implement the DCAVPDP. All instances were run to optimality.

5 Results and Discussion

Table 2 shows the relative performance of the DCAV fleet compared to the single-purpose fleet. The first column features key fleet management performance indicators and the subsequent column "Avg. Diff." shows the overall average performance difference for all instances for both fleets. The columns "BLS", "PPS", "FPS", and "COS" show the performance difference for the corresponding scenarios. The last column shows the number of instances in which better results were achieved using the DCAV fleet. The on-duty utilization rate shows an increase of 4.82% for all scenarios with 241 instances resulting in better values for the DCAV fleet. Most of the performance gain is made in the complementary scenario (COS), where carriers can service both demand types consecutively. The occupancy rate of vehicles is slightly lower for all scenarios, which can be attributed to the increased use of modules and the difference in extra ride times and travel distance when compared to the single-purpose fleet. In 329 instances the percentage of requests served is similar or better than the single-purpose fleet. This difference might be caused by the coupling and decoupling delays of the DCAV fleet, costing additional time and resulting in time windows of requests not being met. Serving fewer requests can also contribute to the −1.30% average decrease in vehicle occupancy. The DCAV fleet show a decrease in the average waiting times of requests, except for the complimentary scenario. The latter can again be attributed to the couple and decouple times of the DCAV fleet, having to switch modules when the generated requests change from passenger to freight requests. Lower waiting times for the other scenarios can be explained by the 7.58% increased use of load-carrying vehicles by the DCAV fleet. When time windows allow, the DCAV fleet uses more modules to be able to handle requests of a similar type more quicker. The complementary scenario (COS) therefore shows a much smaller increase in the number of load-carrying vehicles. The DCAV average fleet size is 18.77% lower, with the complementary scenario (COS) featuring the largest drop—42.60% DCAV are needed. This lower total fleet size is reflected in the total vehicle utilization: the active carriers are used 23.75% more than the active single-purpose AVs.

The average fleet size and total travel distance across scenarios can be seen in Fig. 5. Comparing the number of vehicles shown in the first graph we see that the modular fleet uses more modules of each type while using fewer carriers on average. Due to the coupling and decoupling time, the number of modules might be higher than the equivalent single-purpose vehicles, however, the difference is mostly caused by an increase in the use of passenger modules. Another explanation could be that the modular fleet enables the use of more passenger modules when carriers are available to more quickly serve passenger requests since the model is not minimizing the number of modules used. The difference in total modules used and the number of carriers used does show that the modular system makes use of its flexibility. The lower average travel distance of the modules can be explained by the use of parking locations since modules are being coupled closer to request locations.

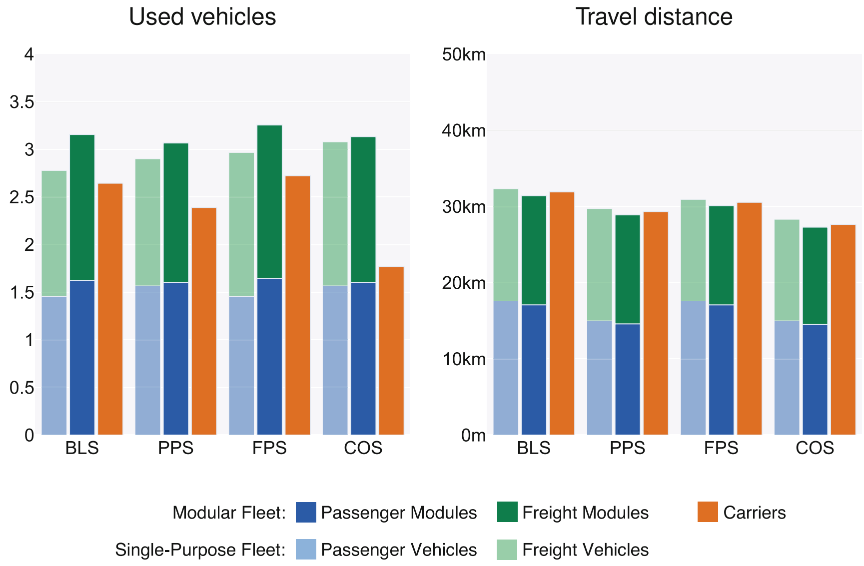

Fig. 5. Average fleet size and distance traveled for all fleet types across the four demand distribution scenarios.

Table 2. Performance difference of the modular DCAV fleet compared to the single-purpose fleet. The final column shows the number of ran instances that show better performance for the DCAV fleet.

Performance Indicator	Avg. Diff	BLS	PPS	FPS	COS	#DCAV best
Utilization rate (on-duty)	4.82%	−4.80%	3.82%	−1.14%	24.36%	241/360
Utilization rate (total)	23.75%	2.90%	16.82%	7.78%	74.71%	326/360
Occupancy rate	−1.30%	−1.49%	−0.47%	−2.35%	−0.97%	240/360
Service rate	−0.08%	−0.15%	0.00%	−0.15%	0.00%	329/360
Avg. pickup time	−9.70%	−22.23%	−10.27%	−8.17%	3.28%	219/360
Avg. ride times	−4.57%	−9.73%	−1.72%	−8.15%	−1.51%	330/360
Fleet capacity	7.58%	13.6%	5.75%	9.74%	1.81%	266/360
Fleet size	−18.77%	−4.80%	−17.62%	−8.24%	−42.60%	346/360
Distance traveled	−1.52%	−1.27%	−1.32%	−1.21%	−2.38%	218/360

6 Conclusion

This study has presented a MILP formulation for the *Dynamically Configurable Autonomous Vehicle Pickup and Delivery Problem* (DCAVPDP). The model provides the first quantitative method investigating the benefits of a DCAV-based transport system, which leverages automation and a novel automotive modular design concept to service multiple demand types by dynamically configuring vehicle upper compartments. We compare the performance of a single-purpose fleet consisting of dedicated passenger and freight vehicles and a DCAV fleet consisting of motorized autonomous carriers and switchable passenger- and freight-tailored compartments to service a mixed pickup and delivery heterogeneous demand comprised of passenger and freight requests considering various scenarios. Since autonomous carriers are expected to be the most expensive component of a DCAVPDP system, we have aimed at achieving high utilization rates for these assets. In total, 360 different instances were run for each fleet configuration. The average performance of all tested mixed-demand scenarios shows an improvement in average modular fleet utilization (carriers coupled to modules) in relation to average single-purpose mixed fleet utilization up to 24.36% when there is a distinct separation between demand types throughout the operation horizon (complementary scenario). The proposed model can be adapted to support more compartment types with varying capacities and features, giving rise to a highly customizable transportation service. Future research will focus on developing a dynamic problem formulation, the adoption of crowd-sourced heterogeneous lower and upper parts, and the repositioning of carriers and modules throughout parking locations anticipating future demand.

References

1. Beirigo, B.A., Schulte, F., Negenborn, R.R.: Integrating people and freight transportation using shared autonomous vehicles with compartments. IFAC-PapersOnLine **51**, 392–397 (2018). https://doi.org/10.1016/j.ifacol.2018.07.064
2. Beirigo, B.A., Schulte, F., Negenborn, R.R.: A learning-based optimization approach for autonomous ridesharing platforms with service-level contracts and on-demand hiring of idle vehicles. Transp. Sci. **56**(3), 677–703 (2022). https://doi.org/10.1287/trsc.2021.1069
3. Cheng, R., Jiang, Y., Nielsen, O.A.: Integrated people-and-goods transportation systems: from a literature review to a general framework for future research, pp. 1–24 (2023). https://doi.org/10.1080/01441647.2023.2189322
4. Continental: Continental launches bee in the urban world of the future (2017). https://www.continental.com/en/press/press-releases/bee-96328. Accessed 28 June 2023
5. Daimler: Vision urbanetic (2019). https://media.mercedes-benz.com/article/c518445b-9050-42ec-9be1-3446e1bf3973. Accessed 28 June 2023
6. Drexl, M.: On some generalized routing problems. Ph.D. thesis, Faculty of Business and Economics, RWTH Aachen (2007). http://publications.rwth-aachen.de/record/62536
7. Hörl, S., Ruch, C., Becker, F., Frazzoli, E., Axhausen, K.: Fleet operational policies for automated mobility: a simulation assessment for Zurich. Transp. Res. Part C: Emerg. Technol. **102**, 20–31 (2019). https://doi.org/10.1016/j.trc.2019.02.020
8. Li, B., Krushinsky, D., Reijers, H.A., Van Woensel, T.: The share-a-ride problem: people and parcels sharing taxis. Eur. J. Oper. Res. **238**(1), 31–40 (2014). https://doi.org/10.1016/j.ejor.2014.03.003
9. Mourad, A., Puchinger, J., Chu, C.: A survey of models and algorithms for optimizing shared mobility. Transp. Res. Part B: Methodol. **123**, 323–346 (2019). https://doi.org/10.1016/j.trb.2019.02.003
10. Münster, M., et al.: U-shift vehicle concept: modular on the road. In: Bargende, M., Reuss, H.-C., Wagner, A. (eds.) 21. Internationales Stuttgarter Symposium.

P, pp. 333–346. Springer, Wiesbaden (2021). https://doi.org/10.1007/978-3-658-33466-6_23

11. Şahin, T., Raulf, C., Kızgın, V., Huth, T., Vietor, T.: A cross-domain system architecture model of dynamically configurable autonomous vehicles. In: Bargende, M., Reuss, H.-C., Wagner, A. (eds.) 21. Internationales Stuttgarter Symposium, pp. 13–31. Springer, Wiesbaden (2021). https://doi.org/10.1007/978-3-658-33521-2_2
12. Sun, S., Wong, Y.D., Liu, X., Rau, A.: Exploration of an integrated automated public transportation system. Transp. Res. Interdisc. Perspect. **8**, 100275 (2020). https://doi.org/10.1016/j.trip.2020.100275
13. van der Tholen, M., Beirigo, B.A., Jovanova, J., Schulte, F.: The share-a-ride problem with integrated routing and design decisions: the case of mixed-purpose shared autonomous vehicles. In: Mes, M., Lalla-Ruiz, E., Voß, S. (eds.) ICCL 2021. LNCS, vol. 13004, pp. 347–361. Springer, Cham (2021). https://doi.org/10.1007/978-3-030-87672-2_23
14. Toyota: E-Pallete (2023). https://www.toyota-europe.com/startyourimpossible/e-palette. Accessed 28 June 2023
15. Ulrich, C., Friedrich, H.E., Weimer, J., Schmid, S.A.: New operating strategies for an on-the-road modular, electric and autonomous vehicle concept in urban transportation. World Electr. Veh. J. **10**(4), 91 (2019). https://doi.org/10.3390/wevj10040091